

Projected Proca Field Theory: a One-Loop Study

R.F. Ozela,^{1,2} Van Sérgio Alves,² E.C. Marino,³ Leandro O. Nascimento,⁴
J.F. Medeiros Neto,² Rudnei O. Ramos,⁵ and C. Morais Smith¹

¹*Institute for Theoretical Physics, Utrecht University, 3584 CC Utrecht, The Netherlands*

²*Faculdade de Física, Universidade Federal do Pará, 66075-110 Belém, PA, Brazil*

³*Instituto de Física, Universidade Federal do Rio de Janeiro, 21941-972 Rio de Janeiro, RJ, Brazil*

⁴*Faculdade de Física, Universidade Federal do Pará, 68800-000 Breves, PA, Brazil*

⁵*Departamento de Física Teórica, Universidade do Estado do Rio de Janeiro, 20550-013 Rio de Janeiro, RJ, Brazil*

The recent discovery of two-dimensional Dirac materials, such as graphene and transition-metal-dichalcogenides, has raised questions about the treatment of hybrid systems, in which electrons moving in a two-dimensional plane interact via virtual photons from the three-dimensional space. In this case, a projected non-local theory, known as Pseudo-QED, or reduced QED, has shown to provide a correct framework for describing the interactions displayed by these systems. In a related situation, in planar materials exhibiting a superconducting phase, the electromagnetic field has a typical exponential decay that is interpreted as the photons having an effective mass, as a consequence of the Anderson-Higgs mechanism. Here, we use an analogous projection to that used to obtain the pseudo-QED to derive a Pseudo-Proca equivalent model. In terms of this model, we unveil the main effects of attributing a mass to the photons and to the quasi-relativistic electrons. The one-loop radiative corrections to the electron mass, to the photon and to the electron-photon vertex are computed. In particular, we calculate the g -factor and show that it diverges when the photon and electron masses are equal, while it retrieves the results obtained for graphene within Pseudo-QED in the limit when both masses vanish.

I. INTRODUCTION

The use of Quantum Field Theories (QFT) to describe two-dimensional systems has gained increased attention during the last years. This is due to the great agreement obtained between the theoretical predictions and the experimental data in many condensed-matter systems. Examples range from the integer and the fractional quantum Hall effects [1–5] to the study of transport in graphene [6–14], excitonic properties of Transition Metal Dichalcogenides (TMDs) [15–17] and superconductivity in layered materials [18–22].

Among those, a particular interest is devoted to the so-called Dirac systems, which exhibit quasi-relativistic dynamics, with massless (e.g., graphene) or massive (e.g., silicene and TMDs) electrons moving with the Fermi velocity. These Dirac materials then operate as QFT laboratories [23].

The description of the electron-electron interactions in planar materials is rather involved because the photons mediating the interactions live in (3+1)D, whereas the electron-dynamics is constraint to a two-dimensional spatial plane. The appropriate theory to capture this electron-photon dimensional mismatch is the so called pseudo-quantum electrodynamics (PQED) [24] (sometimes also named reduced-QED [25–27]). In this approach, a projected electromagnetic field emulates the properties of the (3+1)D photons.

The PQED has been demonstrated to be unitary [28], local [29] and has been successfully applied to describe several properties of graphene. Among others, we highlight the Fermi velocity renormalization in the absence [12] or in the presence [14] of a magnetic field in the vicinity of a conducting plate [30] or in a cav-

ity [31]. In addition, it provided a theoretical description of the Quantum Valley Hall Effect, quantum corrections for the longitudinal conductivity in graphene [13], and of the corrections to the electron's g -factor due to interactions [32]. When accounting for massive electrons, the theory was shown to describe the excitonic spectrum in TMDs [16] and dynamical chiral symmetry breaking [33]. A dual PQED type of model describing the interaction between point vortex excitations and with some interesting properties has also been recently constructed [34].

Another topic that attracted much attention recently is the superconductivity that shows up at low temperatures in bilayer graphene twisted at the *magic* angle ($\theta \approx 1.1^\circ$) [35, 36].

An interesting related question is how to treat a decaying magnetic field due to the presence of superconductivity in that case. The characteristic Meissner-Ochsenfeld magnetic field screening in superconductors is usually described by massive photons (e.g., as described by using the Ginzburg-Landau equations in three-spatial dimensions). Such a model, however, lacks the projection component to describe planar relativistic condensed-matter systems, which are accounted for within the PQED.

Here, we will follow steps similar to the ones that led to the construction of the PQED model [24] and develop a theory to describe electron-electron interactions through a *massive* vector (Proca) field. We consider the Proca model in the present work without concern as to the origin of the mass term, which can come from a Higgs-like mechanism for example, in a more fundamental theory (see also, e.g., Refs [34, 37] for other alternative ways of assigning a mass for the gauge fields, but leading to a different dynamics with respect to the present model). Then, we will constrain only the matter (electrons) cur-

rent to the spatial xy plane. The corresponding quantum partition functional is defined initially in 3+1-dimensions and then the third spatial dimension is integrated out. This procedure is very much analogous to the one that links the (3+1)D Maxwell model to the 2+1-dimensions PQED model.

This work is organized as follows. In Sec. II we present the model used in this work and we derive its planar dimensional reduction in a procedure analogous to that used to derive the PQED model. In Sec. III, we compute the electron and photon self-energies for the model, as well as the interaction vertex, within the leading order (one-loop) level. In this same section, we also explicitly derive the g -factor for our model. A comparison of our results with previous ones, when considering the massless regime, is also performed. In Sec. IV we present our conclusions. Some technical details of the calculation of the g -factor are give in the App. A.

II. PSEUDO PROCA MODEL

Let us first consider the (3+1)D Proca (P) model, including the coupling to a general conserved current J^μ . The quantum partition functional is

$$Z_P[J^\mu] = \int \mathcal{D}A_\mu \exp(iS_P), \quad (2.1)$$

where A_μ is a (3+1)D massive vector field and S_P is the action, given by

$$S_P = \int d^4\chi \left(-\frac{1}{4} F_{\mu\nu} F^{\mu\nu} + \frac{m^2}{2} A^\mu A_\mu - e A_\mu J^\mu \right), \quad (2.2)$$

where $F_{\mu\nu} = \partial_\mu A_\nu - \partial_\nu A_\mu$ and m is the vector field mass. Natural units ($\hbar = c = 1$) are considered for the remainder of this section. The vector field propagator is directly derived from Eq. (2.2),

$$G_P^{\mu\nu}(\chi - \chi') = \int \frac{d^4k}{(2\pi)^4} \frac{e^{-ik \cdot (\chi - \chi')}}{k^2 - m^2} \left[\eta^{\mu\nu} - \frac{k^\mu k^\nu}{m^2} \right], \quad (2.3)$$

with χ and χ' representing points in the (3+1)D spacetime and $\eta^{\mu\nu} = \text{diag}(+, -, -, -)$ is the metric tensor. Integrating out the vector field in Eq. (2.1), we obtain

$$Z_P[J^\mu] = Z_0 e^{-i \frac{e^2}{2} \int d^4\chi d^4\chi' J_\mu(\chi) G_P^{\mu\nu}(\chi - \chi') J_\nu(\chi')}, \quad (2.4)$$

where Z_0 is a normalization constant, independent of J^μ . Note that by the conservation of the current, $\partial_\mu J^\mu = 0$, the last term in Eq. (2.3) ($k^\mu k^\nu / m^2$) vanishes in Eq. (2.4).

By using the constrain of having only currents in the xy plane, we can explicitly write the current J^μ as

$$J^\mu(\chi) = \begin{cases} \mathcal{J}^{\hat{\mu}}(t, x, y) \delta(z), & \text{if } \mu = 0, 1, 2, \\ 0, & \text{if } \mu = 3, \end{cases} \quad (2.5)$$

where the hat over an index notation is used to identify objects that assume three values, i.e., $\hat{\mu} = 0, 1, 2$.

After the integration in z and z' space coordinates, Eq. (2.4) can be written as

$$Z_{PP}[\mathcal{J}] = Z_0 e^{-i \frac{e^2}{2} \int d^3\zeta d^3\zeta' J_{\hat{\mu}}(\zeta) G_P^{\hat{\mu}\hat{\nu}}(\zeta - \zeta') J_{\hat{\nu}}(\zeta')}, \quad (2.6)$$

with ζ and ζ' denoting points in the 2+1-dimensions spacetime and $G_P^{\hat{\mu}\hat{\nu}}(\zeta - \zeta')$ is given by

$$G_P^{\hat{\mu}\hat{\nu}}(\zeta - \zeta') = i \int \frac{d^4k}{(2\pi)^4} \frac{\eta^{\hat{\mu}\hat{\nu}}}{k^2 - m^2} e^{-ik \cdot (\chi - \chi')} \Big|_{z=z'=0}, \quad (2.7)$$

where the momentum integration is over the energy-momentum four-vector k^μ .

If we now perform the integration over the third component of k^μ , i.e., k_z , in Eq. (2.7) and hence restrict the dynamics to the xy -space plane, we obtain

$$G_P^{\hat{\mu}\hat{\nu}}(\zeta - \zeta') = \frac{i}{2} \int \frac{d^3k}{(2\pi)^3} \frac{\eta^{\hat{\mu}\hat{\nu}} e^{-ik \cdot (\zeta - \zeta')}}{\sqrt{k^2 - m^2}}, \quad (2.8)$$

with k now indicating a three-vector, stressing the fact that we are now working in the reduced space (effectively, in 2+1-dimensions). However, the above result can also be obtained if we start from a completely 2+1-dimensions, in principle nonlocal, model from the very beginning. We will name this model the ‘‘Pseudo Proca’’ (PP) model, in analogy with the case of the PQED model. The Lagrangian density for this model is expressed as

$$\mathcal{L}_{PP} = -\frac{1}{2} \frac{F_{\hat{\mu}\hat{\nu}} F^{\hat{\mu}\hat{\nu}}}{\sqrt{-\square - m^2}} - e A_{\hat{\mu}} \mathcal{J}^{\hat{\mu}} - \frac{m^2}{2} \frac{A_{\hat{\mu}} A^{\hat{\mu}}}{\sqrt{-\square - m^2}}, \quad (2.9)$$

with $\mathcal{J}^{\hat{\mu}}$ being the general 2+1-dimensions current defined in Eq. (2.5) and \square the d’Alembertian operator (which must be understood as a convolution). The free propagator associated with \mathcal{L}_{PP} is simply given by Eq. (2.8), as can be easily verified. Thus, we immediately realize that

$$G_{PP}^{\hat{\mu}\hat{\nu}}(\zeta - \zeta') = G_P^{\hat{\mu}\hat{\nu}}(\chi - \chi') \Big|_{z=z'=0} \quad (2.10)$$

and, therefore, the quantum partition function of the Pseudo-Proca and that of the (3+1)D Proca models are completely equivalent, as long as the currents of the latter are constrained to a plane, such as in Eq. (2.5).

III. RADIATIVE CORRECTIONS

In this section, we consider a soft symmetry-breaking term in the Dirac action through the Fermi velocity v_F , in order to reproduce the Dirac-like low-energy electronic dispersion. The Lagrangian density in the now 2+1-dimensional Minkowski space is then given by

$$\begin{aligned} \mathcal{L} = & -\frac{1}{2} \frac{F_{\mu\nu} F^{\mu\nu}}{\sqrt{-\square - m^2}} - \frac{m^2}{2} \frac{A^\mu A_\mu}{\sqrt{-\square - m^2}} \\ & + \bar{\psi} (i\gamma^0 \partial_0 + i v_F \gamma^i \partial_i - M c^2) \psi - e \bar{\psi} \gamma^0 \psi A_0 \\ & - e \beta_F \bar{\psi} \gamma^i \psi A_i, \end{aligned} \quad (3.1)$$

with ψ a four-component Dirac spinor, $\beta_F = v_F/c$ and M the Dirac fermion mass. In the above equation and from this point on, we have explicitly retrieved the dimension of the speed of light c (but still keeping $\hbar = 1$ units). For convenience, and to avoid overloading the notation, we suppress the hat of the Lorentz index.

The Feynman rules for the model are obtained as usual [38]. The interaction vertex is given by $\Gamma^\alpha = -ie(\gamma^0, \beta_F \gamma^i)$, the fermion propagator is

$$S_F(p) = i \left(\frac{\gamma^0 p_0 + v_F \gamma^i p_i + M c^2}{p_0^2 - v_F^2 \mathbf{p}^2 - M^2 c^4} \right), \quad (3.2)$$

and the massive vector field propagator reads

$$\Delta_{\mu\nu}(p) = -\frac{i\eta_{\mu\nu}}{2\sqrt{p_0^2 - c^2 \mathbf{p}^2 - m^2 c^4}}. \quad (3.3)$$

A. Electron self-energy

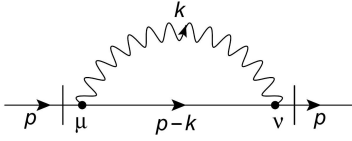


FIG. 1: Feynman Diagram for the one-loop correction to the fermion self-energy.

The electron self-energy at one-loop order is shown in Fig. 1 and the regularized amplitude is given by

$$-i\Sigma(p) = \int \frac{d^D k}{(2\pi)^D} \Gamma^\mu S_F(p-k) \Gamma^\nu \Delta_{\mu\nu}(k), \quad (3.4)$$

where $D = d+1$. In what follows, all momentum integrations in the loop radiative quantities are computed using standard dimensional regularization procedure [39, 40], with $e \rightarrow \mu^{\epsilon/2} e$, $d = 2 - \epsilon$ and μ is the dimensional regularization energy scale.

By substituting the propagators and vertices in Eq. (3.4), we obtain

$$-i\Sigma(p) = \frac{(ie)^2 \mu^\epsilon c}{2} \int \frac{d^D k}{(2\pi)^D} \frac{N_1}{D_1}, \quad (3.5)$$

where N_1 and D_1 are given, respectively, by

$$\begin{aligned} N_1 = & v_F(p-k)_i (\gamma^0 \gamma^i \gamma_0 + \beta_F^2 \gamma^j \gamma^i \gamma_j) \\ & + (p-k)_0 (\gamma^0 \gamma^0 \gamma_0 + \beta_F^2 \gamma^j \gamma^0 \gamma_j) \\ & + M c^2 (\gamma^0 \gamma_0 + \beta_F^2 \gamma^j \gamma_j), \end{aligned} \quad (3.6)$$

$$\begin{aligned} D_1 = & [(p-k)_0^2 - v_F^2 (\mathbf{p}-\mathbf{k})^2 - M^2 c^4] \\ & \times \sqrt{k_0^2 - c^2 \mathbf{k}^2 - m^2 c^4}. \end{aligned} \quad (3.7)$$

Using, hereinafter, the gamma matrix properties $\gamma^0 \gamma_0 = 1$ and $\gamma^j \gamma_j = 2$, we have that

$$-i\Sigma(p) = \frac{(ie)^2 \mu^\epsilon c}{2} \int \frac{dk_0}{2\pi} \frac{d^d k}{(2\pi)^d} \frac{\gamma^0(p-k)_0 (1 + 2\beta_F^2) - v_F \gamma^i(p-k)_i + (1 + 2\beta_F^2) M c^2}{[(p-k)_0^2 - v_F^2 (\mathbf{p}-\mathbf{k})^2 - M^2 c^4] (\sqrt{k_0^2 - c^2 \mathbf{k}^2 - m^2 c^4})}. \quad (3.8)$$

Using the Feynman parameterization,

$$\frac{1}{a\sqrt{b}} = \frac{3}{4} \int_0^1 dx \left\{ \frac{(1-x)^{-1/2}}{[a x + (1-x)b]^{3/2}} \right\}, \quad (3.9)$$

and performing the integration in k_0 , we obtain that Eq. (3.8) can be rewritten as

$$-i\Sigma(p) = \frac{(ie)^2 \mu^\epsilon c}{4\pi} \int_0^1 \frac{dx}{\sqrt{1-x}} \int \frac{d^d k}{(2\pi)^d} \frac{N_2}{D_2}, \quad (3.10)$$

where N_2 and D_2 are defined, respectively, as

$$\begin{aligned} N_2 = & (1 + 2\beta_F^2) M c^2 + (1 - 2\beta_F^2) \gamma^0 p_0 (1-x) \\ & - \left(1 - \frac{v_F^2 x}{\mathcal{B}}\right) v_F \gamma^i p_i, \end{aligned} \quad (3.11)$$

$$D_2 = \mathcal{B} \left[\left(\mathbf{k} - \frac{\mathbf{p} v_F^2 x}{\mathcal{B}} \right)^2 - \frac{\mathbf{p}^2 v_F^4 x^2}{\mathcal{B}^2} + \frac{\mathcal{A}}{\mathcal{B}} \right], \quad (3.12)$$

with \mathcal{A} and \mathcal{B} defined as

$$\mathcal{A} = p_0^2 x^2 + [(M^2 - m^2) c^4 + \mathbf{p}^2 v_F^2 - p_0^2] x + m^2 c^4, \quad (3.13)$$

$$\mathcal{B} = c^2 [1 - x(1 - \beta_F^2)]. \quad (3.14)$$

The electron self-energy then becomes,

$$-i\Sigma(p) = \frac{(ie)^2 c \mu^\epsilon}{4\pi} \int_0^1 \frac{dx}{\mathcal{B} \sqrt{1-x}} \int \frac{d^d k}{(2\pi)^d} \frac{N_2}{k^2 - \Delta}, \quad (3.15)$$

where

$$\Delta = \frac{\mathbf{p}^2 v_F^4 x^2}{\mathcal{B}^2} + \frac{\mathcal{A}}{\mathcal{B}}. \quad (3.16)$$

Performing the integration in the arbitrary dimension $d = 2 - \epsilon$ in Eq. (3.15) in the dimensional regularization procedure, we obtain

$$\begin{aligned} \Sigma(p) &= \frac{(ie)^2 c \mu^\epsilon}{16\pi^2} \int_0^1 \frac{dx}{\sqrt{1-x}} \frac{\Gamma(\frac{\epsilon}{2}) N_2}{\mathcal{B}} \left[\frac{\Delta}{4\pi} \right]^{-\frac{\epsilon}{2}} \\ &= \frac{(ie)^2 c}{16\pi^2} \int_0^1 \frac{dx}{\sqrt{1-x}} \frac{N_2}{\mathcal{B}} \\ &\times \left[\frac{2}{\epsilon} - \gamma_E - \ln \left(\frac{\Delta}{4\pi\mu^2} \right) + \mathcal{O}(\epsilon) \right] \\ &= \Sigma_{\text{finite}}(p) + \Sigma_{\text{div}}(p), \end{aligned} \quad (3.17)$$

where

$$\begin{aligned} \Sigma_{\text{finite}}(p) &= -\frac{(ie)^2 c}{16\pi^2} \int_0^1 \frac{dx}{\sqrt{1-x}} \frac{N_2}{\mathcal{B}} \\ &\times \left[\gamma_E + \ln \left(\frac{\Delta}{4\pi\mu^2} \right) \right] \end{aligned} \quad (3.18)$$

and

$$\Sigma_{\text{div}}(p) = \frac{(ie)^2 c}{8\pi^2 \epsilon} \int_0^1 \frac{dx}{\sqrt{1-x}} \frac{N_2}{\mathcal{B}} \quad (3.19)$$

are the finite and divergent contributions to the electron self-energy, respectively, in the pseudo-Proca QED. One notices that the divergent part of the electron self-energy, Eq. (3.19), is independent of the vector field mass and it is in fact exactly the same result as that obtained in the PQED case [41]. Consequently, the Fermi velocity renormalization will also be the same.

Substituting Eq. (3.11) in Eq. (3.18), we immediately read the one-loop contributions to the electron mass and the wave-function renormalization terms. In particular, the one-loop correction for the fermion mass at zero-external momenta is

$$\begin{aligned} \Sigma_{\text{finite}}^M(0) &= \frac{e^2 c}{16\pi^2} (1 + 2\beta_F^2) M \int_0^1 \frac{dx}{\sqrt{1-x}} \\ &\frac{1}{1-x(1-\beta_F^2)} \left\{ \gamma_E + \ln \left[\frac{M^2 c^2 x + m^2 c^2 (1-x)}{4\pi\mu^2 [1-x(1-\beta_F^2)]} \right] \right\}. \end{aligned} \quad (3.20)$$

The PQED result is obtained by simply setting $m = 0$ in Eq. (3.20). In Fig. 2 we show the behavior of the ratio $\Delta\Sigma^M \equiv [\Sigma_{\text{finite}}^M(0) - \lim_{m \rightarrow 0} \Sigma_{\text{finite}}^M(0)]/(Mc^2)$ as a function of m/M . We note that the electron self-energy correction increases with the vector field mass.

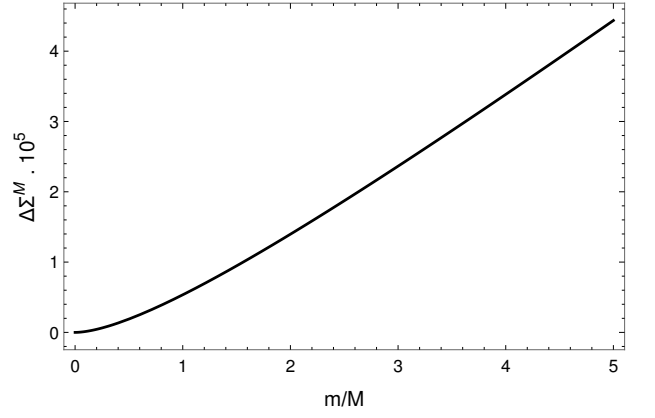


FIG. 2: The difference of the self-energy correction for the fermion mass, with respect to the PQED one, as a function of the mass ratio m/M . For illustrative purposes only, the Fermi velocity was taken to be $v_F = c/300$ and we also have used $e^2 = 4\pi v_F \alpha$, where $\alpha = 1/137$ is the fine-structure constant.

B. The vector field self-energy

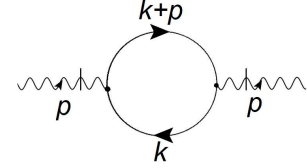


FIG. 3: The one-loop vector field vacuum polarization diagram.

Let us now compute the vector field self-energy, shown in Fig. 3, for the present model. Explicitly, we have that

$$i\Pi^{\mu\nu}(p_0, \mathbf{p}) = - \int \frac{d^D k}{(2\pi)^D} \text{Tr} \left[\Gamma^\mu S_F(k+p) \Gamma^\nu S_F(k) \right]. \quad (3.21)$$

The manipulation of the Dirac algebra proceeds in a standard fashion [38]. Separating the components of the polarization tensor and performing the integration over k_0 and \mathbf{k} in Eq. (3.21), we can write

$$\Pi^{00}(\bar{p}) = \frac{e^2}{8\pi v_F} \left[I_1 + \frac{(\bar{p}^2 - 2p_0^2) I_2}{v_F} + \frac{Mc^2 I_3}{v_F^2} \right], \quad (3.22)$$

$$\begin{aligned} \Pi^{ij}(\bar{p}) &= \frac{e^2 v_F}{8\pi c^2} \left[\left(\frac{\eta^{ij} \bar{p}^2}{v_F^2} - 2p^i p^j \right) I_2 \right. \\ &\quad \left. + \eta^{ij} \left(I_1 + \frac{Mc^2 I_3}{v_F^2} \right) \right], \end{aligned} \quad (3.23)$$

$$\Pi^{0j}(\bar{p}) = -\frac{e^2}{4\pi v_F c} p^0 p^j I_2, \quad (3.24)$$

where for convenience we have introduced the notation $\bar{p} = \sqrt{p_0^2 - v_F^2 \mathbf{p}^2}$ and I_1 , I_2 and I_3 are given, respectively, by

$$I_1 = \frac{1}{v_F} \int_0^1 dx \sqrt{x(1-x)\bar{p}^2 - M^2 c^4}$$

$$= \frac{-i}{8v_F \bar{p}} \left\{ 4Mc^2 \bar{p} + [4M^2 c^4 - \bar{p}^2] \ln \left(\frac{2Mc^2 + \bar{p}}{2Mc^2 - \bar{p}} \right) \right\}, \quad (3.25)$$

$$I_2 = v_F \int_0^1 dx \frac{x(1-x)}{\sqrt{x(1-x)\bar{p}^2 - M^2 c^4}}$$

$$= \frac{i v_F}{8\bar{p}^3} \left\{ 4Mc^2 \bar{p} + [4M^2 c^4 + \bar{p}^2] \ln \left(\frac{2Mc^2 + \bar{p}}{2Mc^2 - \bar{p}} \right) \right\}, \quad (3.26)$$

$$I_3 = \int_0^1 \frac{v_F dx}{\sqrt{x(1-x)\bar{p}^2 - M^2 c^4}} = \frac{i v_F}{\bar{p}} \ln \left(\frac{2Mc^2 + \bar{p}}{2Mc^2 - \bar{p}} \right). \quad (3.27)$$

Notice that the use of the dimensional regularization scheme makes the vector field self-energy explicitly finite. Furthermore, as at the one-loop level the vector field self-energy involves only the electron propagator, the result turns out to be identical to that computed in the context of the 2+1-D QED at one-loop order.

C. Vertex correction and the g -factor

To have a complete one-loop correction analysis, we also compute next the one-loop interaction vertex radiative contribution Γ_{1L}^ν as shown in Fig. 4.

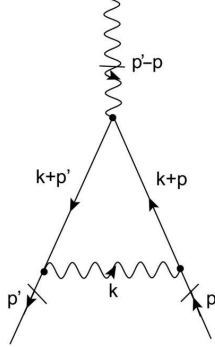


FIG. 4: Feynman diagram for the one-loop correction to the interaction vertex.

Explicitly, Γ_{1L}^ν is given by

$$\Gamma_{1L}^\nu = \int \frac{d^D k}{(2\pi)^D} \Gamma^\alpha S_F(k+p') \Gamma^\nu S_F(k+p) \Gamma^\beta \Delta_{\alpha\beta}(k). \quad (3.28)$$

We will analyze the quantity $M^i = \bar{u}(p') \Gamma^i u(p)$, which relates to the two external fermion lines, $\bar{u}(p')$ and $u(p)$,

in the spatial component of the vertex diagram (because the temporal part of it does not affect the g -factor), such that we can use the Dirac equations to simplify the calculations further.

When represented according to the flux choices in Fig. 4, and after applying a parameterization detailed in the Appendix A, the diagram is written in its parameterized form as

$$M^i = \bar{u}(p') \left(\int_0^1 dx \int_0^{1-x} \frac{dy}{6\pi^2} \frac{M p^i v_F^2}{\sqrt{1-x-y}} \frac{N_3}{\mathcal{K}} \right) u(p), \quad (3.29)$$

with

$$N_3 = \frac{2(1-x-y)\gamma^j \omega_j p_i v_F^2}{\mathcal{D}} - \frac{[\omega_i - 2(x+y)^2 p_i] \beta_F^4}{\mathcal{D}^2}, \quad (3.30)$$

where \mathcal{D} in the above equation is defined as

$$\mathcal{D} = [(1 - \beta_F^2)(x+y) - 1], \quad (3.31)$$

and

$$\mathcal{K} = \mathcal{D}^2 (M^2 c^4 - m^2 c^4 - \omega_0^2) c^2 + [v_F^2 (p' - p)_i^2 + p_0^2] xy$$

$$+ [(x+y)(1-x-y)c^2] (p' + p)_\mu^2 + p_0^2 y^2, \quad (3.32)$$

where $\omega_0 = x p'_0 + y p_0$ and $\omega_i = x p'_i + y p_i$. Then, we detach the terms proportional to $\sigma^{i\alpha}$ from Eq. (3.29) using Gordon decomposition to select the terms M_g^i that are relevant to the g -factor (for more details, see App. A)

$$M_g^i = \bar{u}(p') \left\{ \int_0^1 dx \int_0^{1-x} \frac{dy}{6\pi^2} \frac{M v_F \sigma^{i\alpha} (p' - p)_\alpha \beta_F^2}{\mathcal{K} \sqrt{1-x-y}} \right.$$

$$\times \left[\frac{2(x+y)}{\mathcal{D}} - \frac{\beta_F^2 (x+y)^2}{\mathcal{D}^2} \right] \left. \right\} u(p), \quad (3.33)$$

where the subscripted g index was used to identify that we are only accounting for $\sigma^{i\alpha}$ terms which contribute to the gyromagnetic factor.

To extract the g -factor, however, a few conditions are also necessary, such as the low-energy approximation ($q^2 \rightarrow 0$) and the mass-shell condition (which for small energy values reads as $v_F \gamma^j p_j \cong M c^2$) [32, 38]. After that, we conveniently define a variable

$$\mathcal{K}' = \{[(x+y)^2 - x-y]v_F^2 - [(1-x-y)^2]c^2\}m^2 c^4$$

$$+ 2\{[(x+y)^2 - x-y]c^2 - 2(x+y)^2 v_F^2\}M^2 c^4, \quad (3.34)$$

so that the relevant parts of the vertex correction M_g^i are reduced to the not really simpler but easier to handle integral

$$M_g^i = \bar{u}(p') \left\{ \frac{1}{6\pi^2} \int_0^1 dx \int_0^{1-x} dy \frac{M^2 c^2 \sigma^{i\alpha} q_\alpha v_F^3}{\mathcal{K}' \sqrt{1-x-y}} \right.$$

$$\times \left[2(x+y)\mathcal{D} - (x+y)^2 v_F^2 \right] \left. \right\} u(p). \quad (3.35)$$

We can also identify the g -factor correction form factor F_2 by comparing Eq. (3.33) to

$$M_g^i = i e \beta \bar{u}(p') \left(\frac{i}{2Mc^2} F_2 v_F \sigma^{i\nu} q_\nu \right) u(p). \quad (3.36)$$

Therefore, F_2 is turned into a combination of the integrals in Eq. (3.33), namely,

$$F_2 = -\frac{1}{1 - \left(\frac{m}{M}\right)^2} \int_0^1 \int_0^{1-x} \frac{dy dx}{\pi^2 \sqrt{1-x-y}} \left(\frac{\beta_F^2}{\mathcal{D}} + \frac{\beta_F^4}{\mathcal{D}^2} \right). \quad (3.37)$$

This integral is related to the one obtained in Ref. [32], but in the present work a contribution from m also appears. We then find

$$F_2 = -\frac{\alpha \beta_F^3}{2\pi \left[1 - \left(\frac{m}{M}\right)^2\right]} \bar{R}, \quad (3.38)$$

with $\alpha = e^2/4\pi v_F$ and

$$\bar{R} = \frac{\sqrt{\beta_F^4 - \beta_F^2} + (1 - 6\beta_F^2 + 4\beta_F^4) \coth^{-1} \left(\frac{\beta_F}{\sqrt{\beta_F^2 - 1}} \right)}{\left(\beta_F \sqrt{\beta_F^2 - 1}\right)^3}.$$

Hence,

$$F_2 = \frac{1}{1 - \left(\frac{m}{M}\right)^2} F_2^{\text{PQED}}, \quad (3.39)$$

where

$$F_2^{\text{PQED}} = -\frac{\alpha \beta_F^3}{2\pi} \bar{R}, \quad (3.40)$$

is the PQED result obtained in Ref. [32]. In the Fig. 5, we illustrate the behavior of the result given by Eq. (3.39) as a function of the vector field mass m .

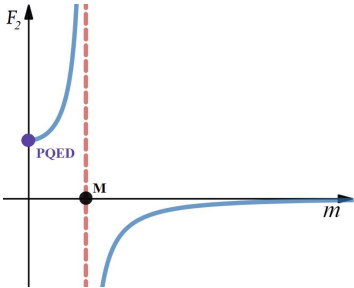


FIG. 5: The g -factor correction (F_2) dependence on the three-dimensional vector field mass m . A divergence occurs when the vector field mass m equals the electron mass M . For $m = 0$, the PQED results are retrieved and for $m \rightarrow \infty$ the g -factor vanishes.

A few predictions emerge from this when looking at some of the limits achievable through the tweak of mass

parameters. The mostly intuitive case occurs when the (3+1)D vector field is heavy with respect to the electron mass, $m \gg M$, which implies in

$$\lim_{\frac{m}{M} \rightarrow \infty} F_2 = 0. \quad (3.41)$$

This could possibly be used to describe systems with a null g -factor [42, 43] (see Fig. 5). The second interesting limit is the expected retrieval of the PQED when m goes to zero (represented by the purple dot in Fig. 5) in the original unprojected model, *i.e.*,

$$\lim_{m \rightarrow 0} F_2 = F_2^{\text{PQED}}. \quad (3.42)$$

Finally, we observe also that the g -factor changes sign as the vector field mass goes from $m < M$ to $m > M$ and that it diverges discontinuously at $m = M$.

IV. CONCLUSIONS

In this work, we have provided a generalization of the dimensional reduction, developed in Ref. [24], for the case of a (3+1)D *massive* vector field. By doing so, we have obtained an effective planar model that retains the fundamental physical properties of the Proca electrodynamics, which is taken as an effective model for describing massive (via the Anderson-Higgs-Meissner mechanism) photons in a material. We have then evaluated the one-loop radiative corrections for the electron and vector field self-energies for this model. We observed that the divergent part of the electron self-energy is exactly identical to the one obtained in the context of the PQED (massless) model. Therefore, from the renormalization group perspective, the renormalization of the Fermi velocity does not depend on the mass of the vector field and, consequently, it is identical to the one obtained for the PQED model [41]. The effective mass for the electron is seen to increase with the vector field mass.

For the vertex diagram, instead, we found that the form factor — and thus this theory's predicted g -factor — depends on the ratio m/M . An unforeseen result arises when the fermion and the photon in the original unprojected model have similar masses (see the region where $m \approx M$ near the red dashed line in Fig. 5), for which the theory predicts a divergent and discontinuous g -factor when $m = M$ and a change of sign. Interestingly, similar effects have been recently found in different materials and have been associated with a so-called giant g -factor [44–46].

Acknowledgments

R.F.O. is partially supported by Coordenação de Aperfeiçoamento de Pessoal de Nível Superior – Brasil (CAPES), finance code 001, and by CAPES/NUFFIC, finance code 0112; V.S.A. is partially supported by

research grants from Conselho Nacional de Desenvolvimento Científico e Tecnológico (CNPq) and by CAPES/NUFFIC, finance code 0112; V.S.A. acknowledges the Institute for Theoretical Physics of Utrecht University for the kind hospitality and M. Gomes for very fruitful discussions; E.C.M. is partially supported by both CNPq and Fundação Carlos Chagas Filho de Amparo à Pesquisa do Estado do Rio de Janeiro (FAPERJ). R.O.R. is partially supported by research grants from CNPq, grant No. 302545/2017-4 and FAPERJ, grant No. E – 26/202.892/2017. J.F.M.N. and R.F.O. are also grateful to M.C. Lima and G.C. Magalhães for very fruitful discussions.

Appendix A: Vertex correction

To shed more light on the g -factor corrections that come from the vertex developed in Subsec. III C, we make the steps that differ from the usual QED more ex-

plicit. The subtlety on the calculation that appears for the model discussed here comes from the fact that it is anisotropic and has a different photon propagator (the planar projection of a massive vector field).

Starting from the vertex structure in Subsec. III C,

$$\Gamma_{1L}^\nu = \int \frac{d^D k}{(2\pi)^D} \Gamma^\alpha \underbrace{S_F(k+p') \Gamma^\nu S_F(k+p)}_{\rho^\nu} \Gamma^\beta \Delta_{\alpha\beta}(k), \quad (\text{A1})$$

we define an auxiliary variable ρ^ν and expand the indices α and β to get

$$\Gamma_{1L}^\nu = \int \frac{d^D k}{(2\pi)^D} [\Gamma^0 \rho^\nu \Gamma^0 \Delta_{00}(k) + \Gamma^l \rho^\nu \Gamma^n \Delta_{ln}(k)]. \quad (\text{A2})$$

In Eq. (A2), the non-diagonal terms of the vector field propagator were dropped because the metrics inside them vanish. Explicitly substituting the Feynman rules given in Sec. III, we find

$$\begin{aligned} \Gamma_{1L}^\nu = & -\frac{ie^2 c}{2} \mu \int \frac{d^D k}{(2\pi)^D} \\ & \left\{ \gamma^0 \left(\frac{\gamma^0(k+p')_0 + v_F \gamma^i(k+p')_i + M c^2}{(k+p')_0^2 - v_F^2(\mathbf{k}+\mathbf{p}')^2 - M^2 c^4} \right) \Gamma^\nu \left(\frac{\gamma^0(k+p)_0 + v_F \gamma^i(k+p)_i + M c^2}{(k+p)_0^2 - v_F^2(\mathbf{k}+\mathbf{p})^2 - M^2 c^4} \right) \gamma^0 \left[\frac{1}{\sqrt{k_0^2 - c^2 \mathbf{k}^2 - m^2 c^4}} \right] + \right. \\ & \left. \beta_F^2 \gamma^l \left(\frac{\gamma^0(k+p')_0 + v_F \gamma^i(k+p')_i + M c^2}{(k+p')_0^2 - v_F^2(\mathbf{k}+\mathbf{p}')^2 - M^2 c^4} \right) \Gamma^\nu \left(\frac{\gamma^0(k+p)_0 + v_F \gamma^i(k+p)_i + M c^2}{(k+p)_0^2 - v_F^2(\mathbf{k}+\mathbf{p})^2 - M^2 c^4} \right) \gamma^n \left[\frac{\eta_{ln}}{\sqrt{k_0^2 - c^2 \mathbf{k}^2 - m^2 c^4}} \right] \right\}. \quad (\text{A3}) \end{aligned}$$

To handle this unusual photon propagator, which contains a square root and a mass term, we apply a slightly modified Feynman parameterization,

$$\frac{1}{abd^{1/2}} = \frac{3}{4} \int_0^1 dx \int_0^{1-x} dy \frac{(1-x-y)^{-1/2}}{[ax+by+d(1-x-y)]^{5/2}} \quad (\text{A4})$$

on the denominator of each term in Eq. (A3). Assuming

$$\begin{aligned} a &= (k+p')_0^2 - v_F^2(\mathbf{k}+\mathbf{p}')^2 - M^2 c^4, \\ b &= (k+p)_0^2 - v_F^2(\mathbf{k}+\mathbf{p})^2 - M^2 c^4, \\ d &= 3k_0^2 - c^2 \mathbf{k}^2 - m^2 c^4, \end{aligned}$$

we find that the denominator of Eq. (A3) is given by

$$\begin{aligned} \frac{1}{abc^{1/2}} = & \frac{3}{4} \int_0^1 dx \int_0^{1-x} dy (1-x-y)^{-1/2} \\ & \{k_0^2(1+x+y) + [2k_0 p'_0 + p'_0{}^2]x \\ & [2k_0 p_0 + p_0^2 - v_F^2(k+p)^2 - M^2 c^4]y + \\ & -c^2 \mathbf{k}^2 - m^2 c^4(1-x-y)\}^{-5/2}. \end{aligned}$$

Now, we complete the k_0 square, make a shift $k_0 \rightarrow k_0 - \omega_0$ (with $\omega_0 = x p'_0 + y p_0$) on it, and solve the integration over k_0 as done in standard anisotropic procedures (at this point, we also drop the odd terms in k_0).

Then, we follow essentially the same steps for \mathbf{k} , but using the shift $\mathbf{k} \rightarrow \mathbf{k} - \boldsymbol{\omega}(\beta_F^2/\mathcal{D}^2)$, with $\mathcal{D} = [(1 - \beta_F^2)(x+y) - 1]$ and $\boldsymbol{\omega} = x \mathbf{p}' + y \mathbf{p}$. Finally, we perform the integration over \mathbf{k} using dimensional regularization [38] to obtain Eq. (3.29), namely:

$$\Gamma_{1L}^i = \int_0^1 dx \int_0^{1-x} \frac{dy}{6\pi^2} \left[\frac{N_3}{\mathcal{K}} \right] \frac{M p^i v_F^2}{\sqrt{1-x-y}}, \quad (\text{A5})$$

where, for convenience, we defined the numerator result for the integration in \mathbf{k} as

$$\begin{aligned} N_3 = & \frac{2(1-x-y)\gamma^j \omega_j p_i v_F^2}{\mathcal{D}} - \frac{[\omega_i - 2(x+y)^2 p_i] \beta_F^4}{\mathcal{D}^2}, \\ \mathcal{D} = & [(1 - \beta_F^2)(x+y) - 1], \end{aligned}$$

and its denominator as

$$\begin{aligned} \mathcal{K} = & \mathcal{D}^2 (M^2 c^4 - m^2 c^4 - \omega_0^2) c^2 + [v_F^2(p' - p)_i^2 + p_0^2] x y \\ & + [(x+y)(1-x-y)c^2] (p' + p)_\mu^2 + p_0^2 y^2. \end{aligned}$$

Using the (Gordon) decomposition identity

$$\bar{u}(p')\gamma^\mu u(p) = \bar{u}(p') \left[\frac{(p' + p)^\mu}{2Mc^2} + i\sigma^{\nu\mu} \frac{q_\nu}{2Mc^2} \right] u(p),$$

where $\bar{u}(p')$ and $u(p)$ are spinorial solutions to the Dirac equations, q_ν is the transferred momentum given by $q_\nu = (p' - p)_\nu$, and $\sigma_{\nu\mu}$ is defined as $\sigma_{\nu\mu} = (i/2)[\gamma_\nu, \gamma_\mu]$, we establish which of the terms of M^i will be relevant to the g -factor. In other words, we select only the terms proportional to $\sigma^{i\alpha}$ from Eq. (3.29) and leave aside the terms that would have a $(p' + p)^\mu$ to define the M_g^i in Eq. (3.33)

$$M_g^i = \bar{u}(p') \left\{ \int_0^1 dx \int_0^{1-x} \frac{dy}{6\pi^2} \frac{M v_F \sigma^{i\alpha} (p' - p)_\alpha \beta_F^2}{\mathcal{K} \sqrt{1-x-y}} \left[\frac{2(x+y)}{\mathcal{D}} - \frac{\beta_F^2 (x+y)^2}{\mathcal{D}^2} \right] \right\} u(p).$$

Applying the same on-shell and low-energy conditions discussed in the Subsec. III C (i.e., $q^2 \rightarrow 0$ and $v_F \gamma^j p_j \cong Mc^2$), \mathcal{K} is changed such that the remaining denominator is now given by

$$\mathcal{K}' = \{[(x+y)^2 - x - y]v_F^2 - [(1-x-y)^2]c^2\}m^2c^4 + 2\{[(x+y)^2 - x - y]c^2 - 2(x+y)^2v_F^2\}M^2c^4.$$

After further simplifications in \mathcal{K}' , we find that both the vector field and the electron masses contribution factorizes from the parametric integrals to yield $1/[1 - (m/M)^2]$ in Eq. (3.37).

-
- [1] T. Ando, Y. Matsumoto, Y. Uemura, *Theory of Hall Effect in a Two-Dimensional Electron System*, Journ. of the Phys. Soc. of Japan **39**, 279 (1975).
 - [2] D.C. Tsui, H.L. Stormer, A.C. Gossard, *Two-Dimensional Magnetotransport in the Extreme Quantum Limit*, Phys. Rev. Lett. **48**, 1559 (1982).
 - [3] R.B. Laughlin, *Anomalous Quantum Hall Effect: An Incompressible Quantum Fluid with Fractionally Charged Excitations*, Phys. Rev. Lett. **50**, 1395 (1983).
 - [4] C.C. Chamon, E. Fradkin, *Distinct universal conductances in tunneling to quantum Hall states: The role of contacts*, Phys. Rev. B **56**, 2012 (1997).
 - [5] O. Heinonen, *Composite Fermions: A Unified View of the Quantum Hall Regime*, World Scientific Pub Co Inc (1998), and articles therein.
 - [6] E.V. Gorbar, V.P. Gusynin, V.A. Miransky, I.A. Shovkovy, *Coulomb interaction and magnetic catalysis in the quantum Hall effect in graphene*, Physica Scripta **T146**, 014018 (2012).
 - [7] I.F. Herbut, *Interactions and Phase Transitions on Graphenes Honeycomb Lattice*, Phys. Rev. Lett. **97**, 146401 (2006).
 - [8] V.P. Gusynin, V.A. Miransky, S.G. Sharapov, I.A. Shovkovy, *Excitonic gap, phase transition, and quantum Hall effect in graphene*, Phys. Rev. B **74**, 195429 (2006).
 - [9] I.F. Herbut, V. Juricic, O. Vafek, *Coulomb Interaction, Ripples, and the Minimal Conductivity of Graphene*, Phys. Rev. Lett. **100**, 046403 (2008).
 - [10] V. Juricic, I.F. Herbut, G.W. Semenoff *Coulomb interaction at the metal-insulator critical point in graphene*, Phys. Rev. B **80**, 081405(R) (2009).
 - [11] M.A.H. Vozmediano, M. I. Katsnelson, F. Guinea, *Gauge fields in graphene*, Physics Reports **496**, 109 (2010).
 - [12] M.A.H. Vozmediano, F. Guinea, *Effect of Coulomb interactions on the physical observables of graphene*, Physica Scripta **T146**, 014015 (2011).
 - [13] E.C. Marino, L.O. Nascimento, V.S. Alves, C.M. Smith, *Interaction Induced Quantum Valley Hall Effect in Graphene*, Phys. Rev. X **5**, 011040 (2015).
 - [14] N. Menezes, V.S. Alves, C.M. Smith *The influence of a weak magnetic field in the Renormalization-Group functions of (2 + 1)-dimensional Dirac systems*, Eur. Phys. J. B **89**, 271 (2016).
 - [15] W. Choi, N. Choudhary, G. H. Han, J. Park, D. Akinwande, Y.H. Lee, *Recent development of two-dimensional transition metal dichalcogenides and their applications*, Materials Today, Volume **20**, 116 (2017).
 - [16] E.C. Marino, L.O. Nascimento, V.S. Alves, N. Menezes, C.M. Smith, *Quantum-electrodynamical approach to the exciton spectrum in transition-metal dichalcogenides*, 2D Materials **5**, 041006 (2018).
 - [17] A.J. Chaves, R.M. Ribeiro, T. Frederico and N.M. R. Peres, *Excitonic effects in the optical properties of 2D materials: an equation of motion approach*, 2D Materials **4**, 025086 (2017).
 - [18] Z. Tesanovic, L. Xing, L. Bulaevskii, Q. Li, M. Suenaga *Critical Fluctuations in the Thermodynamics of Quasi-Two-Dimensional Type-II Superconductors*, Phys. Rev. Lett. **69**, 3563 (1992).
 - [19] S.-C. Zhang, *SO(5) Quantum Nonlinear sigma Model Theory of the High Tc Superconductivity*, Science **275**, 1089 (1997).
 - [20] M. Franz, Z. Tesanovic, O. Vafek, *QED₃ theory of pairing pseudogap in cuprates: From d-wave superconductor to antiferromagnet via an algebraic Fermi liquid*, Phys. Rev. B **66**, 054535 (2002).
 - [21] S.A. Kivelson, I.P. Bindloss, E. Fradkin, V. Oganesyan, J.M. Tranquada, A. Kapitulnik, C. Howald, *Distinct universal conductances in tunneling to quantum Hall states: The role of contacts*, Rev. of Mod Phys. **75**, 2012 (2003).
 - [22] E.C. Marino, D. Niemeyer, V.S. Alves, T. Hansson, S. Moroz, *Screening and topological order in thin superconducting films*, New J. Phys. **20**, 083049 (2018).
 - [23] A.H. Castro Neto, F. Guinea, N.M.R. Peres, K.S. Novoselov, A.K. Geim, *The electronic properties of graphene*, Rev. Mod. Phys. **81**, 109 (2009).
 - [24] E.C. Marino, *Quantum electrodynamics of particles on a plane and the Chern-Simons theory*, Nucl. Phys. B **408**, 551 (1993).
 - [25] E.V. Gorbar, V.P. Gusynin, and V.A. Miransky, *Dynamical chiral symmetry breaking on a brane in reduced QED*, Phys. Rev. D **64**, 105028 (2001).

- [26] S. Teber, *Electromagnetic current correlations in reduced quantum electrodynamics*, Phys. Rev. D **86**, 025005 (2012).
- [27] A.V. Kotikov, S. Teber, *Two-loop fermion self-energy in reduced quantum electrodynamics and application to the ultrarelativistic limit of graphene*, Phys. Rev. D **89**, 065038 (2014).
- [28] E.C. Marino, L.O. Nascimento, V.S. Alves, C.M. Smith, *Unitarity of theories containing fractional powers of the d'Alembertian operator*, Phys. Rev. D **90**, 105003 (2014).
- [29] R.L.P.G. do Amaral and E.C. Marino, *Canonical quantization of theories containing fractional powers of the d'Alembertian operator*, J. of Physics: Mathematical and General **25**, 5183 (1992).
- [30] J.D. Silva, A.N. Braga, W.P. Pires, V.S. Alves, D.T. Alves, E.C. Marino, *Inhibition of the Fermi velocity renormalization in a graphene sheet by the presence of a conducting plate*, Nuclear Physics B **920**, 221 (2017).
- [31] W.P. Pires, J.D. Silva, A.N. Braga, V.S. Alves, D.T. Alves, E.C. Marino, *Cavity effects on the Fermi velocity renormalization in a graphene sheet*, Nuclear Physics B **932**, 529 (2018).
- [32] N. Menezes, V.S. Alves, E.C. Marino, L. Nascimento, L.O. Nascimento, C.M. Smith, *Spin g-factor due to electronic interactions in graphene*, Phys. Rev. B **95**, 245138 (2017).
- [33] V.S. Alves, W.S. Elias, L.O. Nascimento, V. Juricic, F. Peña, *Chiral symmetry breaking in the pseudo-quantum electrodynamics*, Phys. Rev. D **87**, 125002 (2013).
- [34] V.S. Alves, E.C. Marino, L.O. Nascimento, J.F. Medeiros Neto, R.F. Ozela and R.O. Ramos, *Bounded particle interactions driven by a nonlocal dual Chern-Simons model*, arXiv:1901.00513 [hep-th].
- [35] Y. Cao, V. Fatemi, S. Fang, K. Watanabe, T. Taniguchi, E. Kaxiras, P. Jarillo-Herrero, *Unconventional superconductivity in magic-angle graphene superlattices*, Nature **556**, 43 (2018).
- [36] E.F. Talantsev, R.C. Mataira, W.P. Crump, *Classifying superconductivity in magic angle twisted bilayer graphene*, arXiv:1902.07410 [cond-mat.supr-con].
- [37] V.S. Alves, T. Macrì, G.C. Magalhães, E.C. Marino, L.O. Nascimento, *Two-dimensional Yukawa interactions from nonlocal Proca quantum electrodynamics*, Phys. Rev. D **97**, 096003 (2018).
- [38] M.E. Peskin and D.V. Schroeder, *An Introduction to Quantum Field Theory*, Perseus Books Publishing, New York, (1995); M.O.C. Gomes, *Teoria Quântica dos Campos*, Edusp (2002) (in Portuguese).
- [39] C. Bollini, J.J. Giambiagi, *Dimensional Renormalization: The Number of Dimensions as a Regularizing Parameter*, Il Nuovo Cimento B, **12**, 20 (1972).
- [40] G. 't Hooft, M. Veltman, *Regularization and renormalization of gauge fields*, Nuclear Physics B **44**, 189 (1972).
- [41] E.C. Marino, *Quantum Field Theory Approach to Condensed Matter Physics*, Cambridge University Press (2017).
- [42] L.F. Chibotaru, L. Ungur, *Negative g Factors, Berry Phases, and Magnetic Properties of Complexes* Phys. Rev. Letters **109**, 246403 (2012).
- [43] W. Sheng, A. Babinski, *Zero g-factors and nonzero orbital momenta in self-assembled quantum dots*, Phys. Rev. B **75**, 033316 (2007).
- [44] R. Bi, Z. Feng, X. Li, J. Niu, J. Wang, Y. Shi, D. Yu, X. Wu, *Spin zero and large Landé g-factor in WTe₂*, New Journal of Physics **20**, 063026 (2018).
- [45] A. Giorgioni, S. Paleari, S. Cecchi, E. Vitiello, E. Grilli, G. Isella, W. Jantsch, M. Fanciulli, F. Pezzoli, *Giant g-factor tuning of long-lived electron spins in Ge*, Nature Communications **7**, 13886 (2016).
- [46] B. Nedniyom, R.J. Nicholas, M.T. Emeny, L. Buckle, A.M. Gilbertson, P.D. Buckle, T. Ashley, *Giant enhanced g-factors in an InSb two-dimensional gas*, Phys. Rev. B **80**, 125328, (2009).